J Eng Math (2008) 62:373–387
DOI 10.1007/s10665-008-9233-3

A regularization study of some softening beam problems with an implicit gradient plasticity model

Noël Challamel

Received: 10 August 2007 / Accepted: 16 April 2008 / Published online: 16 May 2008

Abstract The modelling of plastic beams experiencing softening is studied. The homogeneous cantilever beam loaded by a concentrated force at its extremity is considered. This simple structural problem with gradient bending moment allows an analytical treatment of the evolution problem. A gradient plasticity model is developed in order to overcome Wood's paradox. Surprisingly, explicit gradient plasticity models do not eliminate this paradox, since the beam response is found to be not continuous with respect to the loading parameter. A new implicit gradient plasticity model is used in this paper. It is shown that the new regularized problem is well-posed. Closed-form solutions of the elastoplastic deflection are finally derived. These results are valid for the beam bending problem, but also for the simple analogy of the bar subjected to distributed axial force.

Keywords Beam · Continuity · Gradient plasticity · Ill-posedness · Non-local · Softening

1 Introduction

Historically, moment–curvature relationships with softening branch were first introduced for reinforced concrete beams. In 1968 Wood did point out some specific difficulties occurring during the solution of the evolution problem for plastic softening models. More precisely, he highlighted the impossibility of the plastic softening beam to flow, a phenomenon sometimes called Wood's paradox. Since this seminal work [1], many papers have been published on softening models (see for instance [2] or the book of Jirasek and Bažant [3] for an extensive review). A lot of non-local models have been developed since the last four decades, and it is expected that the non-local moment–curvature relationship can overcome Wood's paradox.

Integral-type or gradient non-local models abandon the classical assumption of locality, and admit that stress depends not only on the state variables at that point. The first models of this type were applied in the 1960s to the modelling of elastic waves dispersion in crystals. Non-local elasticity was further extended to non-local elastoplasticity by Eringen in the early 1980s [4,5]. Non-local inelastic models (damage or plasticity models) were later successfully used as a localization limiter with a regularization effect on softening structural response. The non-local character of the constitutive law, generally introduced through an internal length, is restricted to the

N. Challamel (✉)
Laboratoire de Génie Civil et de Génie Mécanique, INSA de Rennes, Université Européenne de Bretagne,
20, avenue des Buttes de Coësmes, 35043 Rennes cedex, France
e-mail: noel.challamel@insa-rennes.fr

loading function (damage loading function or plasticity loading function). Pijaudier-Cabot and Bažant [6] elaborated a non-local damage theory, based on the introduction of the non-locality in the damage loading function. This theory has the advantage of leaving the initial elastic behaviour unaffected, and controlling the localization process in the post-peak regime. It is worth mentioning that this idea was already used before to model shear bands [7,8]. Explicit gradient plasticity models, including the numerical implementation in a Finite Element Code, were developed at the beginning of the 1990s [9,10]. The question of defining the non-local variable from the local variable is debated by Peerlings et al. for gradient damage models [11]. The distinction between explicit gradient damage models (the non-local strain is defined explicitly from the local strain and its derivative) and implicit gradient damage models (the non-local strain is obtained implicitly from an integral operator) is established. Following these works devoted to damage models, implicit gradient plasticity models have been also derived by Engelen et al. [12,13]. The theoretical challenges related to these non-local inelastic theories (plasticity or damage) were mainly oriented towards the relevancy of an integral or a gradient-based formulation [14,15], the choice of an explicit or an implicit gradient models [11–13], the justification of relevant boundary conditions associated with the non-local nature of the constitutive law [9,16] or the thermodynamic background of these models [17–19].

Despite the numerous papers devoted to the modelling of softening media with a non-local constitutive law, very few works have been published on the application of such models at the beam scale, or for simple structural members (see also [20] for this problem). Historically, moment–curvature relationships with softening branch were first introduced for reinforced concrete beams. Wood did point out some specific difficulties occurring during the solution of the evolution problem for plastic softening models [1]. More precisely, he highlighted the impossibility of the plastic softening beam to flow, a phenomenon sometimes called Wood's paradox (see also [21]). It is expected that the non-local moment–curvature relationship can overcome Wood's paradox. An explicit gradient plasticity model [9,10], has been considered by Challamel [22] for the beam subjected to a bending moment. However, this gradient plasticity model does not eliminate the ill-posedness of the evolution problem in the presence of a moment gradient (as for instance in the case of homogeneous cantilever beams), since the beam response is not continuous with respect to the loading parameter: Wood's paradox is also encountered for such classical gradient plasticity models, except in some specific inhomogeneous beams [23]. It is worth mentioning that similar difficulties were suggested by Pamin [24] for the three-dimensional problem. We show in this paper that Wood's paradox can be overcome with an implicit gradient plasticity model. The homogeneous cantilever beam loaded by a concentrated force at its extremity is first considered. An implicit gradient plasticity model is developed in order to control the localization process induced by microcracking phenomena. It is shown that the regularized problem is well-posed. Closed-form solutions of the elastoplastic deflection are finally derived. The length of the plastic zone grows during the softening process until an asymptotic limited value, which depends on the characteristic length of the material.

2 The bending problem

A homogeneous cantilever beam of length L is loaded by a vertical concentrated load P at its end (Fig. 1). One recognizes the Galileo cantilever beam previously solved by Galileo himself (1564–1642) using equilibrium, strength and dimensional arguments [25,26]. Of course, no constitutive model was introduced at this early stage. Nevertheless, this pioneering study is often considered as one of the first results of a kinematic method of yield design (see, for instance, [27]). The cantilever beam loaded by a concentrated force can be viewed as a typical case of plastic beams with non-constant bending moment. This plastic softening beam typically models reinforced concrete beams, or steel beams in the presence of local buckling [3,23,28]. The axial and transversal coordinates are denoted by x and y, respectively, and the transverse deflection is denoted by w (Fig. 1). Further, the beam is assumed to be sufficiently restrained in order to prevent lateral–torsional buckling (see the recent papers [29,30] on the modelling of lateral–torsional buckling of cantilever beams). The symmetrical section has a constant second moment of area denoted by I (about the z-axis). We assume that plane cross-sections remain plane and normal to the deflection line and that transverse normal stresses are negligible (Euler–Bernoulli assumption). Accordingly, the curvature χ is related to the deflection through:

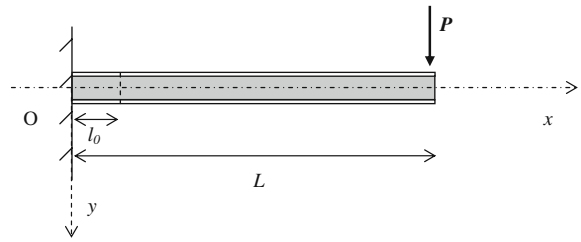

Fig. 1 The cantilever beam

$$\chi(x) = w''(x), \tag{1}$$

where a prime denotes the derivative with respect to x. The problem being statically determinate, equilibrium equations directly give the moment distribution along the beam:

$$M(x) = P(L - x) \text{ with } P \geq 0 \text{ and } x \in [0; L]. \tag{2}$$

At the end of the beam, the displacement of concentrated force P will be denoted by v and used to control the loading process:

$$v = w(L). \tag{3}$$

Accordingly, the loading process is completely specified by the displacement history.

3 Non-local constitutive law

The moment–curvature relationship (M, χ) considered is bilinear with a linear elastic part and a linear non-local curvature-softening part. The moment–curvature relationship for the elastoplastic beam is given by:

$$M = EI(\chi - \chi_p), \tag{4}$$

where E is the Young modulus of the homogeneous beam and χ_p is the plastic curvature.

The elasto-plastic model is a classical plastic model with isotropic negative hardening (softening). The yield function f is given by:

$$f(M, M^*) = |M| - \left(M_p + M^*\right), \tag{5}$$

where M^* is an additional variable which accounts for the loading history, and M_p is the initial plastic bending moment. M^* is related to a non-local plastic curvature variable $\hat{\chi}_p$ through the linear model:

$$M^* = k\hat{\chi}_p, \tag{6}$$

where the plastic modulus k is negative for softening models. A characteristic length l_c is introduced in the definition of the non-local plastic curvature $\hat{\chi}_p$. The definition of this non-local variable depends on the model considered, namely an explicit gradient plasticity model, and an implicit gradient plasticity model (see [12,13,31]). For a homogeneous plastic curvature state, this non-local variable is reduced to the local one $\left(\hat{\chi}_p = \chi_p\right)$.

4 Structural analysis

The maximum bending moment occurs at $x = 0$, where the beam is clamped. Plastic rotation starts as soon as the bending moment reaches the plastic bending moment M_p. The maximum elastic displacement at the beam end v_Y and the corresponding load P_Y are given by:

$$v_Y = \frac{M_p L^2}{3EI} \quad \text{and} \quad P_Y = \frac{M_p}{L}. \tag{7}$$

For a displacement v smaller than $v_Y (v \leq v_Y)$, the beam remains elastic and the deflection can be computed using the elastic solution:

$$v \leq v_Y \Rightarrow EI\, w(x) = -\frac{P}{6}x^3 + PL\frac{x^2}{2} \quad \text{with} \quad P = 3\frac{EI}{L^3}v. \tag{8}$$

The relationship (8) gives the deflection w as a function of the displacement at the end of the beam v which will be used to control the loading process. For $P = P_Y$, we obtain the characteristic deflection $w_Y(x)$:

$$v = v_Y \Rightarrow EI\, w_Y(x) = -\frac{M_p}{6L}x^3 + M_P\frac{x^2}{2}. \tag{9}$$

For v greater than $v_Y (v \geq v_Y)$, the plastic regime starts and the beam can be split into an elastic and a plastic domain. The size of the plastic domain is denoted by $l_0 \leq L$ (see Fig. 1). The governing equations in the plastic domain are:

$$x \in [0; l_0] : \left| \begin{array}{l} EI\left(w^{-\prime\prime}(x) - \chi_p(x)\right) = P\,(L-x) \\ \tilde{\chi}_p(x) = \dfrac{P\,(L-x) - M_p}{k} \end{array} \right. , \tag{10}$$

where w^- denotes the deflection in the plastic region. Moreover, one has to ensure that the plastic curvature evolution is monotonic during the loading. The elastic adjacent domain is governed by:

$$x \in [l_0; L] : EI\, w^{+\prime\prime}(x) = P(L-x); \tag{11}$$

w^+ is the deflection in the elastic region. The boundary conditions can be summarised as:

$$\left| \begin{array}{l} w^-(0) = 0 \\ w^{-\prime}(0) = 0 \end{array} \right. \text{and} \left| \begin{array}{l} w^-(l_0) = w^+(l_0) \\ w^{-\prime}(l_0) = w^{+\prime}(l_0) \end{array} \right. . \tag{12}$$

The deflection $w(x)$ and the rotation $w'(x)$ must be continuous functions of x (in particular at the intersection of the elastic and the plastic domains).

5 Explicit gradient plasticity model

In the explicit gradient plasticity model, the non-local curvature may be defined as:

$$\hat{\chi}_p = \overline{\chi_p} = \chi_p + l_c^2 \chi_p''. \tag{13}$$

This model is called an explicit gradient plasticity model, as the non-local plastic curvature may be directly expressed in terms of the plastic curvature and its derivatives (see [31] for this convention). The boundary conditions are expressed as (see for instance [23]):

$$\chi_p(l_0) = 0, \;\; \chi_p'(l_0) = 0 \quad \text{and} \quad \chi_p'(0) = 0. \tag{14}$$

The plastic curvature and its derivative are assumed to be continuous with respect to the spatial coordinate x. The third boundary condition at the clamped end is the extra boundary condition.

The linear differential equation (10) dealing with χ_p (with the non-local plastic curvature defined in Eq. 13) can be written as:

$$x \in [0; l_0] : \quad \chi_p + l_c^2 \chi_p'' = \frac{P(L-x) - M_p}{k}. \tag{15}$$

The general solution of this differential equation is as follows:

$$\chi_p(x) = A\cos\frac{x}{l_c} + B\sin\frac{x}{l_c} + \frac{P\,(L-x) - M_p}{k}. \tag{16}$$

The three boundary conditions defined by (14) lead to a nonlinear system of three equations with three unknowns A, B and l_0:

$$A\cos\frac{l_0}{l_c} + B\sin\frac{l_0}{l_c} + \frac{P(L-l_0) - M_p}{k} = 0, \quad -\frac{A}{l_c}\sin\frac{l_0}{l_c} + \frac{B}{l_c}\cos\frac{l_0}{l_c} - \frac{P}{k} = 0, \quad \frac{B}{l_c} - \frac{P}{k} = 0. \tag{17}$$

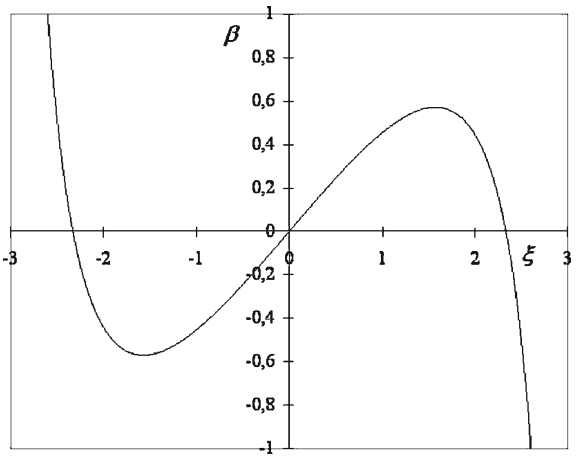

Fig. 2 Apparent hardening process for the explicit softening gradient plasticity model - β versus ξ

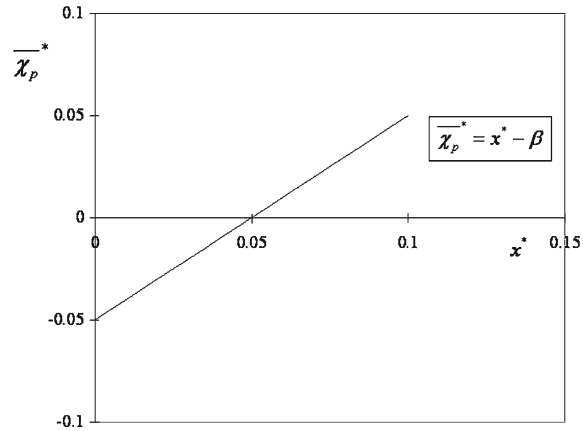

Fig. 3 Possible negative values of the non-local plastic curvature for the explicit gradient plasticity softening model—$\beta = 0.05$ (hardening range)

The following dimensionless parameters may be introduced:

$$\beta = \left(1 - \frac{P_Y}{P}\right)\frac{L}{l_c} \leq 0 \quad \text{and} \quad \xi = \frac{l_0}{l_c} \geq 0. \tag{18}$$

The resolution of the system (17) leads to a relationship between the dimensionless loading parameter β and the dimensionless size of the plastic zone ξ:

$$\beta = \xi + \frac{\cos\xi - 1}{\sin\xi} \qquad \text{for} \quad \sin(\xi) \neq 0. \tag{19}$$

The solution $\xi = 2n\pi$ has to be excluded, as this solution cannot be connected to the elastic solution. An asymptotic expansion for small values of ξ shows that, in this last case:

$$\xi \ll 1 \Rightarrow \beta \sim \frac{\xi}{2}. \tag{20}$$

As a consequence, it is clear that for positive values of ξ, this softening gradient plasticity model leads to a global hardening process in the vicinity of the plastic load P_Y (see Fig. 2):

$$\xi \to 0^+ \Rightarrow \beta \to 0^+. \tag{21}$$

It may be convenient to introduce the dimensionless non-local plastic curvature:

$$x^* \in [0;\xi]: \quad \overline{\chi_p}^*\left(x^*\right) = x^* - \beta(\xi) \quad \text{with} \quad \left| \begin{array}{l} x^* = \dfrac{x}{l_c} \\ \overline{\chi_p}^* = |k|\,\dfrac{\overline{\chi_p}}{P l_c} \end{array} \right. . \tag{22}$$

In this case, for positive values of β (hardening process in the vicinity of the plastic load), the non-local plastic curvature $\overline{\chi_p}$ can take negative values which is not physically admissible (see Fig. 3):

$$\beta \geq 0 \Rightarrow \overline{\chi_p}(0) = \frac{PL - M_p}{k} \leq 0. \tag{23}$$

The only admissible range for β is to take negative values (for the softening problem), and the only admissible range for ξ is to take positive values; however, for $\beta \to 0^-$ it is continuously $\xi < 0$; see Fig. 2). Hence, for β being in the admissible range, ξ is outside its admissible range, and the physically sensible solution with a plastic zone of finite length does not exist. Hence, one cannot connect the elastic and the plastic solution, as shown by Challamel and Hjiaj [23]. As a consequence, Wood's paradox is observed for such explicit gradient plasticity models (see

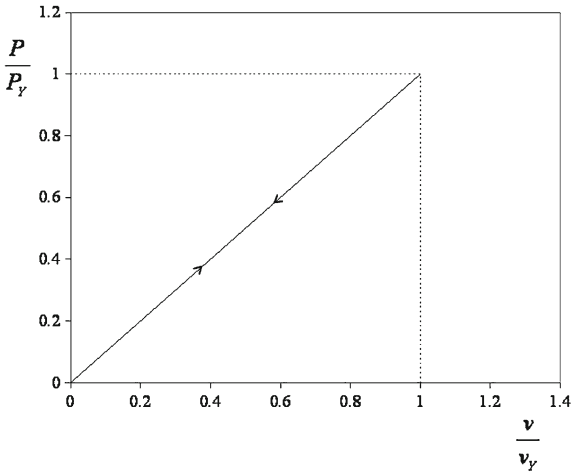

Fig. 4 Wood's paradox—explicit gradient plasticity models

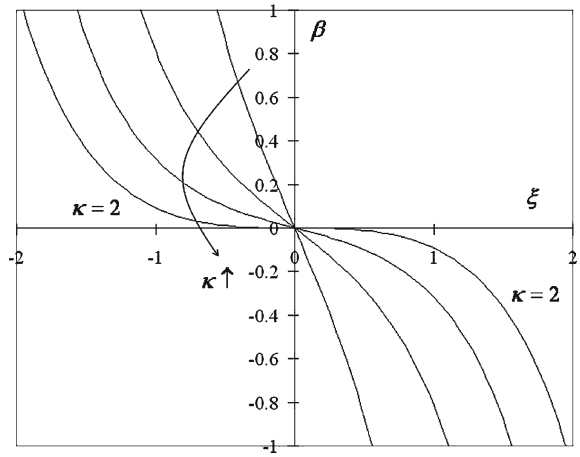

Fig. 5 Evolution of the plastic zone ξ versus the loading parameter β; Softening regularization for $\kappa \in]1;2]$

Fig. 4). Such a paradox can also be observed in the case of a tensile bar under a stress gradient (as considered in [32] for a bar with an inhomogeneous section). It is shown numerically that the tension load increases at the beginning of the plastic process (apparent hardening process), despite the linear intrinsic softening constitutive law. Such a numerical result [32] clearly shows, according to (23), that the non-local plastic strain could be negative, a result which is physically questionable for the tension-loading test. Hence, the specific phenomenon highlighted in this paper for explicit gradient plasticity models has been obtained already in the literature from a numerical point of view.

6 Implicit gradient plasticity model

In the implicit gradient plasticity model, the non-local curvature may be defined as:

$$\hat{\chi}_p = \chi_p + \kappa \left(\overline{\chi_p} - \chi_p \right). \tag{24}$$

It is worth mentioning that such a combination of local and non-local plastic variables was initially proposed by Vermeer and Brinkgreve [33]. The non-local plastic curvature $\overline{\chi_p}$ is defined as the solution of the modified Helmholtz equation:

$$\overline{\chi_p} - l_c^2 \overline{\chi_p}'' = \chi_p. \tag{25}$$

This model depends on a regularization scalar factor κ. The specific case $\kappa = 2$ leads to the simplified formulae:

$$\kappa = 2 \Rightarrow \hat{\chi}_p = \overline{\chi_p} + l_c^2 \overline{\chi_p}''. \tag{26}$$

The boundary conditions are expressed as:

$$\chi_p (l_0) = 0, \ \overline{\chi_p}' (l_0) = 0 \quad \text{and} \quad \overline{\chi_p}' (0) = 0. \tag{27}$$

An important difference with standard implicit gradient plasticity models (see for instance [12,13,31]), however, is that the extra boundary conditions are valid over the plastic domain, rather than over the entire domain (as was also shown by Fleck and Hutchinson [16]). It can be shown that Wood's paradox would also be observed if boundary conditions are applied at the physical boundary of the domain (see Appendix). Hence, the implicit gradient plasticity model considered in this paper can be considered as a new model, which has not yet been studied in the literature.

The system is now solved for the non-local plastic curvature $\overline{\chi_p}$:

$$\overline{\chi_p} + l_c^2 (\kappa - 1) \overline{\chi_p}'' = \frac{P (L - x) - M_p}{k} \tag{28}$$

with the three boundary conditions expressed in term of the unknown variable $\overline{\chi_p}$:

$$\overline{\chi_p}(l_0) - l_c^2 \overline{\chi_p}''(l_0) = 0, \quad \overline{\chi_p}'(l_0) = 0 \quad \text{and} \quad \overline{\chi_p}'(0) = 0. \tag{29}$$

The nature of the differential equation (28) depends on the sign of $\kappa - 1$. The system is first solved when this term is negative ($\kappa < 1$). The general solution of the differential equation (28) is then written as:

$$x \in [0; l_0] : \overline{\chi_p}(x) = A \cosh \frac{x}{l_c\sqrt{1-\kappa}} + B \sinh \frac{x}{l_c\sqrt{1-\kappa}} + \frac{P(L-x) - M_p}{k}. \tag{30}$$

The three boundary conditions defined by Eq. 29 lead to a nonlinear system of three equations with three unknowns A, B and l_0:

$$\begin{aligned} &-\frac{\kappa}{1-\kappa} A \cosh \frac{l_0}{l_c\sqrt{1-\kappa}} - \frac{\kappa}{1-\kappa} B \sinh \frac{l_0}{l_c\sqrt{1-\kappa}} + \frac{P(L-l_0) - M_p}{k} = 0, \\ &\frac{A}{l_c\sqrt{1-\kappa}} \sinh \frac{l_0}{l_c\sqrt{1-\kappa}} + \frac{B}{l_c\sqrt{1-\kappa}} \cosh \frac{l_0}{l_c\sqrt{1-\kappa}} - \frac{P}{k} = 0, \quad \frac{B}{l_c\sqrt{1-\kappa}} - \frac{P}{k} = 0. \end{aligned} \tag{31}$$

The relationship between the dimensionless loading parameter β and the dimensionless size of the plastic zone ξ is found to be:

$$\beta = \xi - \frac{\kappa}{\sqrt{1-\kappa}} \frac{1 - \cosh \frac{\xi}{\sqrt{1-\kappa}}}{\sinh \frac{\xi}{\sqrt{1-\kappa}}}. \tag{32}$$

An asymptotic expansion for small values of ξ shows that, in this last case:

$$\xi \ll 1 \Rightarrow \beta \sim \frac{2-\kappa}{2(1-\kappa)} \xi \quad \text{for} \quad 1 - \kappa > 0. \tag{33}$$

As for the explicit gradient plasticity model, the first-order term in Eq. 33 is positive (apparent hardening process) and Eq. 21 still holds (it could also be shown that the non-local plastic curvature $\overline{\chi_p}$ could be negative in this case). For instance, an asymptotic expansion of the non-local plastic curvature at the clamped end shows that:

$$\xi \ll 1 \Rightarrow \overline{\chi_p}(0) \sim \frac{P l_c}{k} \frac{1}{2(1-\kappa)} \xi < 0 \quad \text{for} \quad 1 - \kappa > 0. \tag{34}$$

This means that Wood's paradox is still observed for such an implicit gradient plasticity model for this range of regularization factor (Fig. 4 is still valid in this case). On the other hand, for positive values of $\kappa - 1$ ($\kappa > 1$), the general solution of the differential equation (28) is written as:

$$x \in [0; l_0] : \overline{\chi_p}(x) = A \cos \frac{x}{l_c\sqrt{\kappa-1}} + B \sin \frac{x}{l_c\sqrt{\kappa-1}} + \frac{P(L-x) - M_p}{k}. \tag{35}$$

The nonlinear system of three equations with three unknowns A, B and l_0 is now written as:

$$\begin{aligned} &\frac{\kappa}{\kappa-1} A \cos \frac{l_0}{l_c\sqrt{\kappa-1}} + \frac{\kappa}{\kappa-1} B \sin \frac{l_0}{l_c\sqrt{\kappa-1}} + \frac{P(L-l_0) - M_p}{k} = 0, \\ &-\frac{A}{l_c\sqrt{\kappa-1}} \sin \frac{l_0}{l_c\sqrt{\kappa-1}} + \frac{B}{l_c\sqrt{\kappa-1}} \cos \frac{l_0}{l_c\sqrt{\kappa-1}} - \frac{P}{k} = 0, \quad \frac{B}{l_c\sqrt{\kappa-1}} - \frac{P}{k} = 0 \end{aligned} \tag{36}$$

and the load-plastic-zone relationship is finally written as:

$$\beta = \xi - \frac{\kappa}{\sqrt{\kappa-1}} \frac{1 - \cos \frac{\xi}{\sqrt{\kappa-1}}}{\sin \frac{\xi}{\sqrt{\kappa-1}}} \quad \text{for} \quad \sin\left(\frac{\xi}{\sqrt{\kappa-1}}\right) \neq 0. \tag{37}$$

The solution $\xi = 2n\pi\sqrt{\kappa-1}$ has to be excluded, as this solution cannot be connected to the elastic solution. The asymptotic expansion for small values of ξ shows that, in this last case:

$$\xi \ll 1 \Rightarrow \beta \sim \frac{2-\kappa}{2\,(1-\kappa)} \xi \quad \text{for} \quad 1 - \kappa < 0. \tag{38}$$

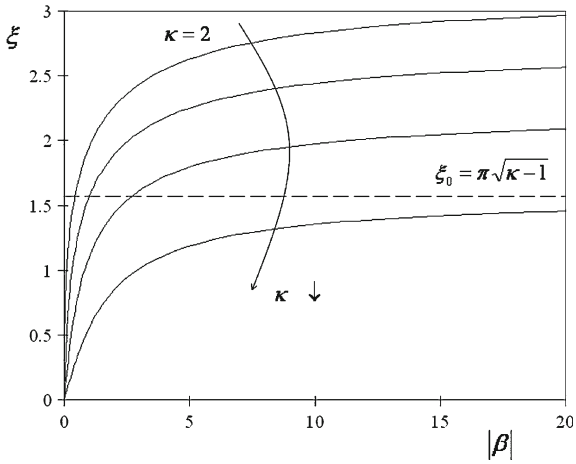

Fig. 6 Evolution of the plastic zone ξ versus the loading parameter β; $\kappa \in]1; 2]$

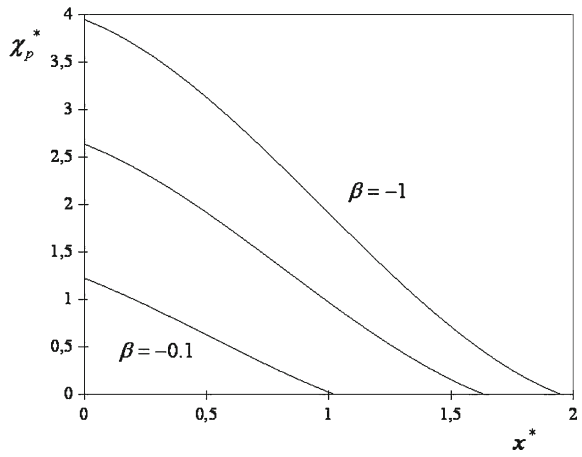

Fig. 7 Evolution of the plastic curvature χ_p^* for three loading cases—$\kappa = 2$

Equation 38 is identical with Eq. 33, meaning that the first-order term does not depend on the sign of $1 - \kappa$. The interesting result is that the first-order term may take negative values for $\kappa \in]1; 2]$; see also Fig. 5. In this case, for β being in the admissible range, ξ is inside its admissible range, and the plastic zone may spread; see also Fig. 5:

$$\xi \to 0^+ \Rightarrow \beta \to 0^-. \tag{39}$$

Therefore, the connection of the elastic and the plastic solution is implicitly fulfilled with this regularization method. A second-order analysis would show that the case $\kappa = 2$ can be included in the analysis:

$$\kappa = 2 \Rightarrow \beta = \xi - 2\frac{1 - \cos\xi}{\sin\xi} \sim -\frac{\xi^3}{12} \quad \text{for} \quad \xi \ll 1. \tag{40}$$

In other words, Wood's paradox may be overcome by taking κ larger than unity. Furthermore, we will show that uniqueness prevails for the softening evolution considered in the paper, and the softening problem is clearly regularized for $\kappa \in]1; 2]$.

Figure 6 shows the evolution of the plastic zone ξ in term of the positive dimensionless parameter $|\beta|$. The parameter $|\beta|$ varies between 0 and tends towards an infinite value when P tends towards zero. For each value of the regularization parameter κ, there is only one curve crossing the origin which relates the plastic zone to the loading parameter. This means that the regularized problem becomes well-posed. It has to be recalled that a well-posed problem (in the Hadamard sense) is a problem which has at least one solution (existence of the solution) and at most one solution (uniqueness) [34]. Moreover, the size of the plastic zone tends towards an asymptotic value for large values of $|\beta|$ (and sufficiently small values of P):

$$\xi_0 = \pi\sqrt{\kappa - 1} \quad \text{for} \quad \kappa > 1. \tag{41}$$

7 Resolution of the cantilever case

The solution of the plastic curvature in the plastic zone can finally be written as:

$$x^* \in [0; \xi]: \quad \chi_p^*(x^*) = -\frac{\kappa}{\sqrt{\kappa - 1}} \frac{\cos\frac{\xi}{\sqrt{\kappa-1}} - 1}{\sin\frac{\xi}{\sqrt{\kappa-1}}} \cos\frac{x^*}{\sqrt{\kappa - 1}} - \frac{\kappa}{\sqrt{\kappa - 1}} \sin\frac{x^*}{\sqrt{\kappa - 1}} + x^* - \beta(\xi)$$

$$\text{with} \left| \begin{array}{l} x^* = \dfrac{x}{l_c} \\ \chi_p^* = |k| \dfrac{\chi_p}{P l_c} \end{array} \right., \tag{42}$$

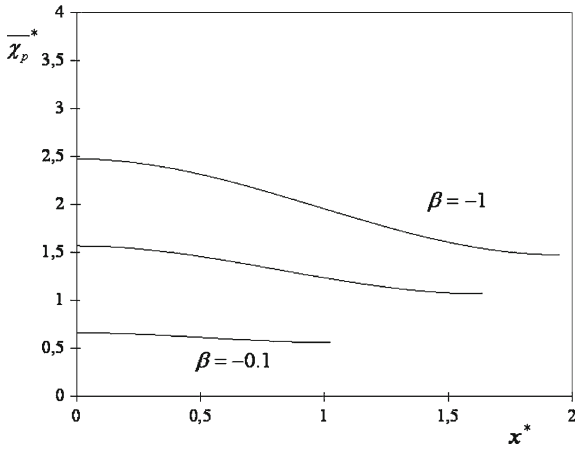

Fig. 8 Evolution of the non-local plastic curvature $\overline{\chi_p}^*$ for three loading cases—$\kappa = 2$

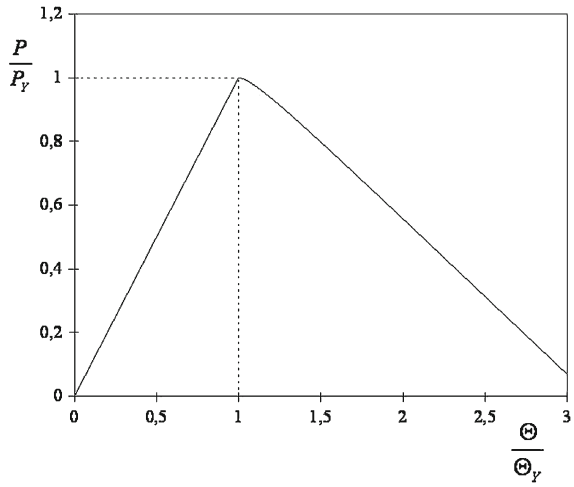

Fig. 9 Response of the elastoplastic beam $\frac{P}{P_Y}$ versus $\frac{\Theta}{\Theta_Y}$ $-\kappa = 2$; $\frac{EI}{k} = -5$; $\frac{l_c}{L} = 0.1$

where ξ is computed from β (or P) from Eq. 37. The size of the plastic zone increases as $|\beta|$ increases and the monotonic assumption of plastic growth can be checked (see for instance Fig. 7). In Fig. 7, the slope at the origin of the plastic curvature function appears to differ significantly from zero (as assumed in the explicit gradient plasticity model). The numerical case treated in Fig. 7 is based on $\kappa = 2$ and then, $\xi_0 = \pi$.

It is interesting to notice that the non-local plastic curvature is not continuous at the boundary between the plastic and the elastic zones (see Fig. 8). The non-local plastic curvature grows linearly in the plastic zone:

$$x^* \in [0;\xi]: \quad \overline{\chi_p}^*\left(x^*\right) = -\sqrt{\kappa-1}\frac{\cos\frac{\xi}{\sqrt{\kappa-1}}-1}{\sin\frac{\xi}{\sqrt{\kappa-1}}}\cos\frac{x^*}{\sqrt{\kappa-1}} - \sqrt{\kappa-1}\sin\frac{x^*}{\sqrt{\kappa-1}} + x^* - \beta(\xi)$$

$$\text{with } \overline{\chi_p}^* = \frac{\overline{\chi_p}}{Pl_c}|k|\,. \tag{43}$$

The rotation function $\theta(x)$ (or $w'(x)$) is calculated from integration of the differential equation:

$$\theta'(x) = \chi_p(x) + \frac{P(L-x)}{EI} \quad \text{with} \quad \theta(0) = 0. \tag{44}$$

The rotation in the plastic zone is obtained from:

$$\theta^-(x) = P\left(\frac{1}{EI}+\frac{1}{k}\right)\left(Lx-\frac{x^2}{2}\right) - \frac{M_p}{k}x + \kappa\frac{Pl_c^2}{k}\frac{\cos\left(\frac{l_0}{l_c\sqrt{\kappa-1}}\right)-1}{\sin\left(\frac{l_0}{l_c\sqrt{\kappa-1}}\right)}\sin\left(\frac{x}{l_c\sqrt{\kappa-1}}\right)$$

$$-\kappa\frac{Pl_c^2}{k}\left[\cos\left(\frac{x}{l_c\sqrt{\kappa-1}}\right)-1\right]. \tag{45}$$

The rotation in the elastic zone is derived from the continuity of the rotation along the elastoplastic boundary (see Eq. 12):

$$\theta^+(x) = \frac{PL}{EI}(x-l_0) - \frac{P}{2EI}\left(x^2-l_0^2\right) + \theta^-(l_0)\,. \tag{46}$$

The rotation at the end of the beam is denoted by Θ (and $\Theta_Y = P_Y L^2/2EI$). The relationship between this normalized rotation and the loading parameter is simplified in

$$\frac{\Theta}{\Theta_Y} = \frac{P}{P_Y} + \frac{2EI}{k}\left(\frac{l_0}{L}\frac{P}{P_Y} - \frac{P}{2P_Y}\left(\frac{l_0}{L}\right)^2 - \frac{l_0}{L}\right). \tag{47}$$

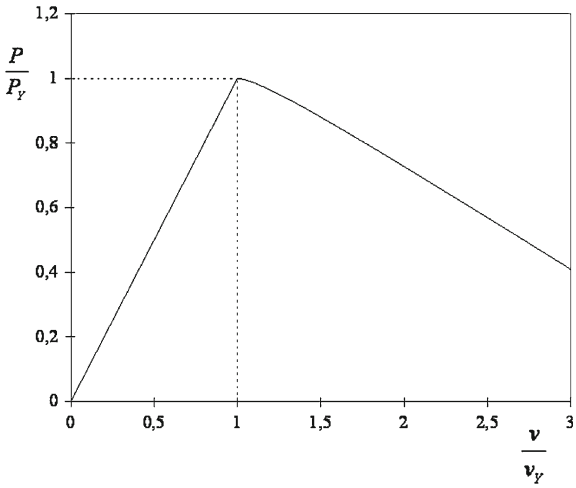

Fig. 10 Response of the elastoplastic beam $\frac{P}{P_Y}$ versus $\frac{v}{v_Y} - \kappa = 2$; $\frac{EI}{k} = -5$; $\frac{l_c}{L} = 0.1$

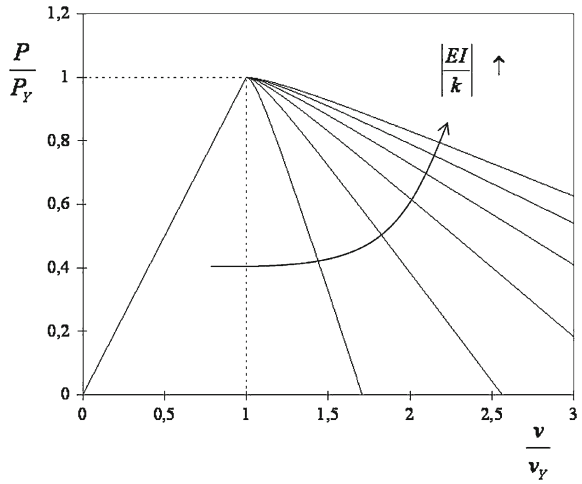

Fig. 11 Influence of the stiffness ratio on the response of the elastoplastic beam $\frac{P}{P_Y}$ versus $\frac{v}{v_Y}$ -; $\kappa = 2$; $\frac{l_c}{L} = 0.1$

An example of softening response is shown in Fig. 9 for the load-rotation response. The regularization of the implicit gradient plasticity model is longer more ambiguous. The deflection in the plastic zone is obtained by integrating the rotation given by Eq. 45:

$$w^-(x) = \left(\frac{PL}{EI} + \frac{PL - M_p}{k}\right)\frac{x^2}{2} - \left(\frac{P}{EI} + \frac{P}{k}\right)\frac{x^3}{6}$$
$$-\kappa\sqrt{\kappa-1}\frac{Pl_c^3}{k}\frac{\cos\left(\frac{l_0}{l_c\sqrt{\kappa-1}}\right)-1}{\sin\left(\frac{l_0}{l_c\sqrt{\kappa-1}}\right)}\left[\cos\left(\frac{x}{l_c\sqrt{\kappa-1}}\right)-1\right] - \kappa\frac{Pl_c^2}{k}\left[l_c\sqrt{\kappa-1}\sin\left(\frac{x}{l_c\sqrt{\kappa-1}}\right)-x\right]. \quad (48)$$

The deflection in the elastic zone is derived from the continuity condition given by Eq. 12:

$$w^+(x) = \frac{PLx^2}{2EI} - \frac{Px^3}{6EI} + \left[w^{-\prime}(l_0) - \frac{PLl_0}{EI} + \frac{Pl_0^2}{2EI}\right]x + \left[w^-(l_0) - l_0 w^{-\prime}(l_0) + \frac{PLl_0^2}{2EI} - \frac{Pl_0^3}{3EI}\right]. \quad (49)$$

The evolutions of the deflection are shown on Figs. 10–13. The global ductility increases as the stiffness ratio $|EI/k|$ increases, or the length ratio l_c/L increases. Moreover, the regularization parameter κ controls the beginning of the softening regime($\kappa \in]1; 2]$). A flat transition with a horizontal tangency corresponds to κ equal to 2.

8 Constant bending moment

The implicit gradient plasticity model is also studied in case of constant bending moment ($M(x) = \Gamma$). The beam may also be split into a plastic zone and an elastic one, as shown in Fig. 14 (see also [22]):

$$x \in [0; l_0] : \overline{\chi_p} + l_c^2(\kappa-1)\overline{\chi_p}'' = \frac{\Gamma - M_p}{k} \quad \text{with} \quad \overline{\chi_p}(l_0) - l_c^2\overline{\chi_p}''(l_0) = 0, \quad \overline{\chi_p}'(l_0) = 0 \quad \text{and} \quad \overline{\chi_p}'(0) = 0. \quad (50)$$

In this case, the plastic zone does not evolve, and is given for $\kappa > 1$ by

$$\xi = n\pi\sqrt{\kappa-1} \quad \text{with} \quad \xi = \frac{l_0}{l_c} \geq 0, \quad (51)$$

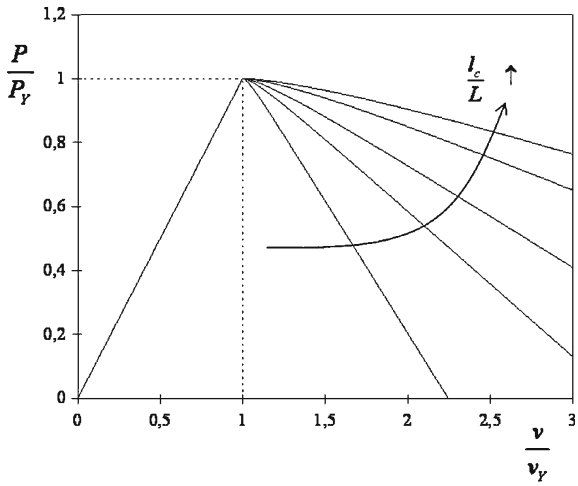

Fig. 12 Influence of the characteristic length on the response of the elastoplastic beam $\frac{P}{P_Y}$ versus $\frac{v}{v_Y}$ $-\kappa = 2$; $\frac{EI}{k} = -5$

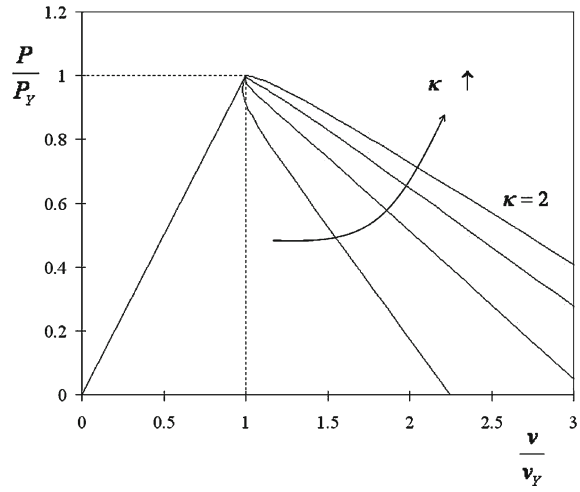

Fig. 13 Influence of the regularization parameter κ on the response of the elastoplastic beam $\frac{P}{P_Y}$ versus $\frac{v}{v_Y}$ $-\frac{l_c}{L} = 0.1$; $\frac{EI}{k} = -5$ and $\kappa \in]1; 2]$

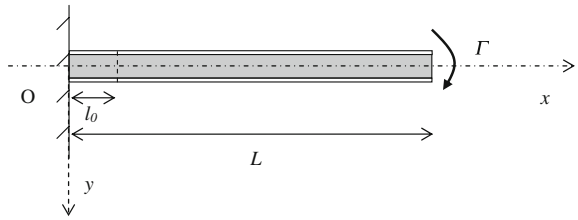

Fig. 14 Beam under constant bending moment

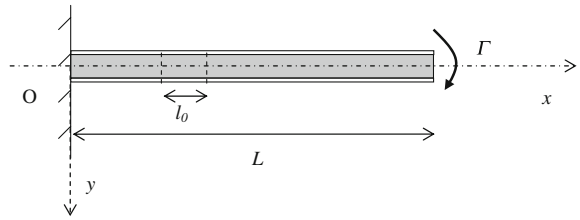

Fig. 15 Beam under constant bending moment—Non-uniqueness of the solution

where n is an integer. The number n of solutions to take into account depends on the total length of the beam. It is remarkable that the plastic length associated with n equal to 1 is the one asymptotically obtained in presence of moment gradient (see Eq. 41). The plastic curvature is finally obtained from

$$\chi_p^*\left(x^*\right) = 1 - (-1)^n \cos\left(\frac{x^*}{\sqrt{\kappa - 1}}\right) \quad \text{with} \quad \left| \begin{array}{l} x^* = \dfrac{x}{l_c} \\ \chi_p^* = k\dfrac{\chi_p}{\Gamma - M_p} \end{array} \right. \tag{52}$$

and the non-local plastic curvature is written as

$$\overline{\chi_p}^*\left(x^*\right) = 1 - (-1)^n \frac{\kappa - 1}{\kappa} \cos\left(\frac{x^*}{\sqrt{\kappa - 1}}\right). \tag{53}$$

However, for the specific case of constant bending moment, the problem is generally still ill-posed as the system possesses an infinite number of solutions, in addition to the homogeneous one. It is sufficient to notice that the plastic zone can move along the beam, as suggested by Fig. 15 (in this case, when the plastic zone is free on both sides, the size of the dimensionless plastic zone ξ is equal to $2n\pi\sqrt{\kappa - 1}$ with n integer). This structural case can be understood as a degenerate case from a mathematical point of view, linked to reasons of symmetry.

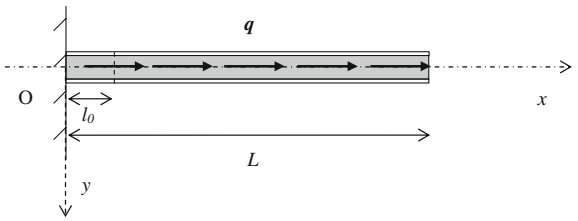

Fig. 16 Bar under distributed axial force

9 Bar under normal force. Analogy

As remarked for instance by Bažant and Zubelewicz [20], a direct analogy between the beam problem and the bar problem may be found. The direct analogue of the bending problem with linearly varying bending moment is the bar problem with distributed axial force (see Fig. 16). In this case, the normal force N varies linearly:

$$N(x) = q(L - x) \tag{54}$$

with q being the uniformly distributed axial force. The constitutive relationship, analogous to Eq. 4 for the bending problem, is given by

$$N = ES(\varepsilon - \varepsilon_p), \tag{55}$$

where S is the cross-section area, ε is the total strain, and ε_p is the plastic strain. The yield function and the gradient plasticity model follow from Eq. 5 and Eq. 6:

$$f(N, N^*) = |N| - \left(N_p + N^*\right) = 0 \quad \text{with} \quad N^* = k\hat{\varepsilon}_p = k\left[\overline{\varepsilon_p} + (\kappa - 1)\, l_c^2 \overline{\varepsilon_p}''\right]; \kappa > 1. \tag{56}$$

The boundary conditions in the plastic zone are written as follows

$$\varepsilon_p\,(l_0) = 0, \quad \overline{\varepsilon_p}'\,(l_0) = 0 \quad \text{and} \quad \overline{\varepsilon_p}'\,(0) = 0. \tag{57}$$

The relationship between the plastic length and the loading parameter is given by Eq. 37, with the following notation:

$$\beta = \left(1 - \frac{q_Y}{q}\right)\frac{L}{l_c} \leq 0, \quad q_Y = \frac{N_p}{L} \quad \text{and} \quad \xi = \frac{l_0}{l_c} \geq 0. \tag{58}$$

The solution of the plastic strain in the plastic zone is similar to that of Eq. 42:

$$x^* \in [0;\xi]: \quad \varepsilon_p^*\left(x^*\right) = -\frac{\kappa}{\sqrt{\kappa-1}}\frac{\cos\frac{\xi}{\sqrt{\kappa-1}} - 1}{\sin\frac{\xi}{\sqrt{\kappa-1}}}\cos\frac{x^*}{\sqrt{\kappa-1}} - \frac{\kappa}{\sqrt{\kappa-1}}\sin\frac{x^*}{\sqrt{\kappa-1}} + x^* - \beta(\xi)$$
$$\text{with} \left| \begin{array}{l} x^* = \frac{x}{l_c} \\ \varepsilon_p^* = |k|\,\frac{\varepsilon_p}{q l_c} \end{array} \right. . \tag{59}$$

The axial displacement in the plastic zone is similar to the rotation in the bending problem $\left(\chi(x) = \theta'(x)\right)$:

$$\varepsilon(x) = u'(x). \tag{60}$$

The axial displacement at the end of the bar $u\,(x = L)$ is denoted by U (and $U_Y = q_Y L^2/2ES$). Hence, the softening curve q/q_Y versus U/U_Y, is obtained from Fig. 9, by replacing P/P_Y by q/q_Y, and Θ/Θ_Y by U/U_Y.

10 Generalisation to three-dimensional media

The one-dimensional implicit gradient plasticity model presented in this paper may be easily extended to three-dimensional media. The yield function f given by Eq. 5 can be generalized by

$$f\left(\underline{\underline{\sigma}}, \underline{\underline{\sigma}}^*\right) = \tilde{\sigma} - \left(\sigma_Y + \tilde{\sigma}^*\right) \quad \text{with} \quad \tilde{\sigma}^* = k\hat{\varepsilon}_p. \tag{61}$$

In this expression, σ_Y and k denote the initial yield stress and the plastic modulus (k is negative for softening models); $\tilde{\sigma}$ is an equivalent stress and $\tilde{\sigma}^*$ is an additional variable which accounts for the loading history; $\tilde{\sigma}^*$ is related to a non-local effective plastic strain variable $\hat{\varepsilon}_p$, defined by

$$\hat{\varepsilon}_p = \overline{\varepsilon_p} + (\kappa - 1)\, l_c^2 \nabla^2 \overline{\varepsilon_p} \quad \text{with} \quad \kappa > 1, \tag{62}$$

where ∇^2 denotes the Laplacian operator. The non-local effective plastic strain is defined as the solution of the modified Helmholtz equation:

$$\overline{\varepsilon_p} - l_c^2 \nabla^2 \overline{\varepsilon_p} = \tilde{\varepsilon}_p. \tag{63}$$

Here $\tilde{\varepsilon}_p$ denotes the usual effective plastic strain. The homogeneous natural boundary conditions hold:

$$\tilde{\varepsilon}_p = 0 \quad \text{or} \quad \underline{n}.\underline{\nabla}\overline{\varepsilon_p} = 0. \tag{64}$$

It is worth mentioning that the thermodynamic background of such a model has not yet been established, and is still an open problem to our knowledge. In the case of a moving internal elasto-plastic boundary, both boundary conditions of Eq. 64 hold. We insist upon the fact that the present boundary conditions must be applied at the elastic–plastic boundary, and not at the external boundary of the problem, as postulated by most standard implicit gradient plasticity models. The main reason is that Wood's paradox would be observed if boundary conditions are postulated at the physical boundary of the body (see the Appendix).

11 Conclusions

This paper deals with the modelling of plastic beams experiencing softening. The homogeneous cantilever beam loaded by a concentrated force at its extremity has been considered. A gradient plasticity model has been developed in order to overcome Wood's paradox. Surprisingly, explicit gradient plasticity models may not eliminate this paradox, since the beam response is found not to be continuous with respect to the loading parameter for softening evolutions. This phenomenon is well understood, from an asymptotic expansion. It is shown, in case of explicit gradient plasticity models, that the non-local plastic curvature could have negative values for a tension bar, a phenomenon which is not acceptable from a physical point of view.

A new implicit gradient plasticity model has been presented in this paper. It has been shown that the new regularized problem is well-posed for specific values of a regularization parameter, denoted by κ. It is probable that the well-posedness of the evolution problem, strongly dependent on the value of the κ-parameter, should also depend on the structural case studied. The cantilever case can be understood at this stage as an elementary structural case, with moment gradient (or with stress gradient for a more general three-dimensional body). In a certain sense, the cantilever-beam analysis developed in this paper closes the discussion of implicit versus explicit gradient plasticity models. It is also shown that the boundary conditions of such an implicit gradient plasticity model have to be postulated at the elastic–plastic boundary in order to overcome Wood's paradox.

Closed-form solutions of the elastoplastic deflection were finally derived. As a consequence of this model, the plastic length evolves during the loading process, a phenomenon often noticed in structural design. These results are valid for the beam-bending problem, but also for the simple analogy of a bar subjected to distributed axial forces (or more generally with linearly varying stress). The present implicit gradient plasticity model has to be computed within a general finite-element framework when dealing with more complex structural systems. An important task is the development of a variational approach including such non-standard boundary conditions for the implicit gradient plasticity model. This topic and the thermodynamics background of the presented model are currently under investigation.

Appendix: On Wood's paradox for some standard implicit gradient plasticity models

The standard implicit gradient plasticity model is studied in this appendix. The differential equation of the non-local plastic curvature $\overline{\chi_p}$ is given by Eq. 28:

$$\overline{\chi_p} + l_c^2 (\kappa - 1) \overline{\chi_p}'' = \frac{P(L-x) - M_p}{k} \quad \text{with} \quad \kappa > 1 \tag{A.1}$$

with the three boundary conditions,

$$\chi_p(l_0) = 0, \quad \overline{\chi_p}'(L) = 0 \quad \text{and} \quad \overline{\chi_p}'(0) = 0. \tag{A.2}$$

The relationship between the local plastic curvature χ_p and the non-local plastic curvature $\overline{\chi_p}$ can be found in Eq. 25. Note the fundamental difference with the boundary conditions expressed by Eq. 27. In the standard implicit gradient plasticity models ([12,13] or [31]), the condition at the boundary of the elastoplastic region $\left(\overline{\chi_p}'(l_0) = 0\right)$ is replaced by a condition at the physical boundary of the body $\left(\overline{\chi_p}'(L) = 0\right)$. The general solution of the differential equation Eq. (A.1) is given by Eq. 35:

$$x \in [0; l_0] : \overline{\chi_p}(x) = A \cos \frac{x}{l_c\sqrt{\kappa - 1}} + B \sin \frac{x}{l_c\sqrt{\kappa - 1}} + \frac{P(L-x) - M_p}{k}. \tag{A.3}$$

The nonlinear system of three equations with three unknowns A, B and l_0 is now written as

$$\left| \begin{array}{l} \dfrac{\kappa}{\kappa - 1} A \cos \dfrac{l_0}{l_c\sqrt{\kappa - 1}} + \dfrac{\kappa}{\kappa - 1} B \sin \dfrac{l_0}{l_c\sqrt{\kappa - 1}} + \dfrac{P(L-l_0) - M_p}{k} = 0, \\ -\dfrac{A}{l_c\sqrt{\kappa - 1}} \sin \dfrac{L}{l_c\sqrt{\kappa - 1}} + \dfrac{B}{l_c\sqrt{\kappa - 1}} \cos \dfrac{L}{l_c\sqrt{\kappa - 1}} - \dfrac{P}{k} = 0, \quad \dfrac{B}{l_c\sqrt{\kappa - 1}} - \dfrac{P}{k} = 0. \end{array} \right. \tag{A.4}$$

The following dimensionless parameters may be introduced:

$$\beta = \left(1 - \frac{P_Y}{P}\right) \frac{L}{l_c} \leq 0, \quad \xi = \frac{l_0}{l_c} \geq 0 \quad \text{and} \quad L^* = \frac{L}{l_c} \tag{A.5}$$

and the load-plastic zone relationship is finally written as

$$\beta = \xi - \frac{\kappa}{\sqrt{\kappa - 1}} \frac{\cos \frac{\xi - L^*}{\sqrt{\kappa - 1}} - \cos \frac{\xi}{\sqrt{\kappa - 1}}}{\sin \frac{L^*}{\sqrt{\kappa - 1}}} \quad \text{for} \quad \sin\left(\frac{L^*}{\sqrt{\kappa - 1}}\right) \neq 0. \tag{A.6}$$

It can be checked that (A.6) and (37) are identical when the elastoplastic boundary and the physical boundary of the beam can be merged ($\xi = L^*$). However, it is not possible to connect the elastic and the plastic solution for the standard implicit gradient plasticity model:

$$\xi = 0 \Rightarrow \beta\,(\xi = 0) = -\frac{\kappa}{\sqrt{\kappa - 1}} \frac{\cos \frac{L^*}{\sqrt{\kappa - 1}} - 1}{\sin \frac{L^*}{\sqrt{\kappa - 1}}}. \tag{A.7}$$

As a consequence,

$$\lim_{\xi \to 0} \beta(\xi) \neq 0 \tag{A.8}$$

Therefore, Wood's paradox is also met for standard implicit gradient plasticity models presented in [12,13] or [31].

References

1. Wood RH (1968) Some controversial and curious developments in the plastic theory of structures. In: Heyman J, Leckie FA (eds) Engineering plasticity. Cambridge University Press, UK, pp 665–691
2. Bažant ZP (1976) Instability, ductility and size effect in strain-softening concrete. J Eng Mech ASCE 102:331–344
3. Jirásek M, Bažant ZP (2002) Inelastic analysis of structures. Wiley

4. Eringen AC (1981) On nonlocal plasticity. Int J Eng Sci 19:1461–1474
5. Eringen AC (1983) Theories of non-local plasticity. Int J Eng Sci 21:741–751
6. Pijaudier-Cabot G, Bažant ZP (1987) Nonlocal damage theory. J Eng Mech 113:1512–1533
7. Aifantis EC (1984) On the microstructural origin of certain inelastic models. J Eng Mater Technol ASME 106:326–330
8. Zbib H, Aifantis EC (1988) On the localization and post-localization behaviour of plastic deformation. I, II, III. Res Mech 23: 261–277;279–292;293–305
9. Mühlhaus HB, Aifantis EC (1991) A variational principle for gradient plasticity. Int J Solids Struct 28:845–857
10. de Borst R, Mühlhaus HB (1992) Gradient-dependent plasticity: formulation and algorithmic aspects. Int J Numer Methods Eng 35:521–539
11. Peerlings RHJ, de Borst R, Brekelmans WAM, de Vree JHP (1996) Gradient-enhanced damage for quasi-brittle materials. Int J Numer Methods Eng 39:3391–3403
12. Engelen RAB, Geers MGD, Baaijens FPT (2003) Nonlocal implicit gradient-enhanced elasto-plasticity for the modelling of softening behaviour. Int J Plasticity 19:403–433
13. Engelen RAB, Fleck NA, Peerlings RHJ, Geers MGD (2006) An evaluation of higher-order plasticity theories for predicting size effects and localisation. Int J Solids Struct 43:1857–1877
14. Huerta A, Pijaudier-Cabot G (1994) Discretization influence on regularization by two localization limiters. J Eng Mech 120(6): 1198–1218
15. Bažant ZP, Jirásek M (2002) Nonlocal integral formulations of plasticity and damage: Survey of progress. J Eng Mech 128:1119–1149
16. Fleck NA, Hutchinson JW (2001) A reformulation of strain gradient plasticity. J Mech Phys Solids 49:2245–2271
17. Benvenuti E, Borino G, Tralli A (2002) A thermodynamically consistent nonlocal formulation for damaging materials. Eur J Mech A/Solids 21:535–553
18. Jirásek M, Rolshoven S (2003) Comparison of integral-type nonlocal plasticity models for strain-softening materials. Int J Eng Sci 41:1553–1602
19. Polizzotto C (2007) Strain-gradient elastic-plastic material models and assessment of the higher order boundary conditions. Eur J Mech A/Solids 26:189–211
20. Bažant ZP, Zubelewicz A (1988) Strain-softening bar and beam: exact non-local solution. Int J Solids Struct 24(7):659–673
21. Royer-Carfagni G (2001) Can a moment–curvature relationship describe the flexion of softening beams. Eur J Mech A/Solids 20:253–276
22. Challamel N (2003) Une approche de plasticité au gradient en construction métallique. Comptes-Rendus Mécanique 331(9): 647–654
23. Challamel N, Hjiaj M (2005) Non-local behavior of plastic softening beams. Acta Mech 178:125–146
24. Pamin J (1994) Gradient-dependent plasticity in numerical simulation of localization phenomena, Dissertation, Delft University of Technology, Delft. Available from http://www.library.tudelft.nl/dissertations.
25. Galileo, Discorsi e Dimonstrazioni Matematiche, intorno à due nuove Scienze, 1638, In: Sur les épaules des géants – les plus grands textes de physique et d'astronomie (Hawkings, S.), pp 154–182. Dunod, 2002
26. Timoshenko SP (1983) History of strength of materials. Dover Publications.
27. Salençon J (1990) An introduction to the yield design theory and its application to soil mechanics. Eur J Mech A/Solids 9(5):477–500
28. Challamel N, Pijaudier-Cabot G (2006) Stability and dynamics of a plastic softening oscillator. Int J Solids Struct 43:5867–5885
29. Challamel N (2007) Lateral-torsional buckling of beams under combined loading—a reappraisal of the Papkovitch-Schaefer theorem. Int J Struct Stab Dyn 7(1):55–79
30. Challamel N, Andrade A, Camotim D (2007) An analytical study on the lateral–torsional buckling of linearly tapered cantilever strip beams. Int J Struct Stab Dyn 7(3):441–456
31. Peerlings RHJ (2007) On the role of moving elastic-plastic boundaries in strain gradient plasticity. Model Simul Mater Sci Eng 15:109–120
32. de Borst R, Pamin J (1996) Some novel developments in finite element procedures for gradient-dependent plasticity. Int J Numer Methods Eng 39:2477–2505
33. Vermeer PA, Brinkgreve RBJ (1994) In: Chambon R, Desrues J, Vardoulakis I (eds) A new effective non-local strain measure for softening plasticity. Rotterdam, Balkema, pp 89–100
34. Tikhonov AN, Arsenine VY (1977) Solutions to ill-posed problems. Winston-Wiley, New-York